Activation of CCR2+ human proinflammatory monocytes by human herpesvirus-6B chemokine N-terminal peptide

D. J. Clark[1], J. Catusse[1, 2], A. Stacey[3], P. Borrow[3] and U. A. Gompels[1]*

[1]Pathogen Molecular Biology Department, London School of Hygiene and Tropical Medicine, University of London, Keppel St., London, UK WC1E 7HT; [2] University Clinic of Freiburg, Department of Hematology and Oncology, Freiburg, Germany, [3] Nuffield Department of Clinical Medicine, University of Oxford, UK

Running title: virus chemokine peptide activates CCR2+ monocytes

* Corresponding author: Dr Ursula Gompels, Pathogen Molecular Biology Department, London School of Hygiene and Tropical Medicine, University of London, Keppel St., London WC1E 7HT, UK. Email: ursula.gompels@lshtm.ac.uk ;Tel: +44 (0)20 79272315

Keywords: virus chemokine, CCR2, chemotaxis, macrophage, inflammation

Word and figure counts: Summary (Abstract): 206; Text: 4250; Figs and tables: 6

ABSTRACT

Human monocytes expressing CCR2 with CD14 or CD16 can mediate antigen presentation and promote inflammation, brain infiltration and immunosenescence. Recently identified roles are in HIV, parasitic and TB disease. Human herpesvirus 6B, HHV-6B, encodes a chemokine, U83B, mono-specific for CCR2; distinct from related HHV-6A U83A, which activates CCR1, CCR4, CCR5, CCR6 and CCR8 on immune effector cells and dendritic cells. These differences could alter leukocyte-subset recruitment for latent/lytic replication and associated neuroinflammatory pathology. Therefore, cellular interactions between U83A and U83B could help dictate potential tropism differences between these viruses. U83A specificity is maintained in the 38-residue N-terminal spliced-truncated form. Here we sought to determine the basis for the chemokine receptor specificity differences and identify possible applications. To do this we first analysed variation in a natural host population in sub-Saharan Africa where both viruses are equally prevalent and compared these to global strains. Analyses of U83 N-terminal variation in 112 HHV-6A and HHV-6B infections identified 6/38 U83A or U83B-specific residues. We also identified a unique single U83A-specific substitution in one U83B sequence, 'U83BA'. Next, the variation effects were tested by deriving N-terminal (NT) 17-mer peptides and assaying activation of *ex vivo* human leukocytes, the natural host and cellular target. Chemotaxis of CCR2+ leukocytes was potently induced by U83B-NT, but not U83BA-NT or U83A-NT. Analyses of the U83B-NT activated population identified migrated CCR2+, but not CCR5+, leukocytes. The U83BA-NT asparagine-lysine14 substitution disrupted activity, defining CCR2 specificity and a main determinant for HHV-6A/B differences in cellular interactions. A flow cytometry-based shape-change assay was designed, and used to provide further evidence that U83B-NT could activate CCR2+CD14+CD16+ monocytes. This defines a potential anti-viral target for HHV-6A/B disease and novel peptide immunomodulator for proinflammatory monocytes.

INTRODUCTION

Human monocytes can be classified into at least two distinct groups, classical and non-classical based on CD14 and CD16 expression. These monocyte subsets express chemokine receptors CCR2 and CX3CR1, respectively, which direct specific tissue migration toward sites of selective chemokine secretion during infection (Ziegler-Heitbrock *et al.*, 2010). Recent studies have defined an intermediate monocyte group with intermediate CD14 and CD16 expression as well as intermediate levels of chemokine receptor expression (Balboa *et al.*, 2011; Buckner *et al.*, 2011; Chimma *et al.*, 2009; Lentz *et al.*, 2011; Williams *et al.*, 2012; Ziegler-Heitbrock *et al.*, 2010). Transcriptome profiling of this group has characterised these as antigen presenting cells with unique proinflammatory properties (Merino *et al.*, 2011; Wong *et al.*, 2011; Zawada *et al.*, 2011; Ziegler-Heitbrock *et al.*, 2010). Therefore the inflammatory response is fine-tuned depending on activation of specific monocyte subsets. Recent evidence demonstrates monocytes in blood expressing CD14, CD16 and CCR2, unlike classical or non-classical monocytes, have roles in mediating HIV migration across the blood brain barrier and in increasing the severity of TB and cardiovascular disease (Balboa *et al.*, 2011; Buckner *et al.*, 2011; Lentz *et al.*, 2011; Williams *et al.*, 2012; Ziegler-Heitbrock *et al.*, 2010). These proinflammatory roles are combined with increased antigen presentation in pleural effusions for TB, improved parasite inhibition, and increased MHC class II and accessory molecules in donor gene expression studies (Balboa *et al.*, 2011; Chimma *et al.*, 2009; Wong *et al.*, 2011; Zawada *et al.*, 2011). Moreover, it has been demonstrated that CD14, CD16, CCR2 expressing monocytes are senescent monocytes, with shortened telomeres and increased chemokine receptor expression, which may characterise increased inflammatory disease in the elderly including disposition to cardiovascular disease (Merino *et al.*, 2011).

Human herpesvirus 6 is a ubiquitous pathogen in many populations, yet virus reactivations from latent infection can be associated with severe inflammatory disease in immunosuppressed patient populations, including post-transplant acute limbic encephalitis (PALE), and cognitive impairment in hematopoietic stem cell transplantation as well as myocarditis (Kuhl *et al.*, 2005a; Kuhl *et al.*, 2005b; Noutsias *et al.*, 2011; Schmidt-Hieber *et al.*, 2011; Seeley *et al.*, 2007; Zerr *et al.*, 2011). By 2 years of age over 75% of infants have acquired this pathogen and in adults HHV-6 seroprevalence is 83-100% worldwide (Hall *et al.*, 2006). Primary infections of infants result in a usually self-limited fever and 10-24% develop a skin rash; *exanthem subitum*, also called roseola (Hall *et al.*, 2006; Hall *et al.*, 1994; Zerr *et al.*, 2005). Recent evidence shows that approximately 0.1-1% of populations examined have integrated HHV-6 genomes in the germline, giving inherited, chromosomally integrated virus, ciHHV-6, with the potential to express virus genes as human alleles in every cell (Arbuckle *et al.*, 2010; Arbuckle & Medveczky, 2011; Morissette & Flamand, 2010), with implications for inflammatory disease.

HHV-6 is comprised of two variants, HHV-6A and HHV-6B, which have been recently classified as distinct species (Adams & Carstens, 2012). They are highly similar in terms of genome size, composition and structure, although there are differences in pathology, cell tropism, and geographic distribution. Primary infant infections in Europe, USA and Japan are predominantly infections with HHV-6B, 97-100%, while in Africa the reverse has been found; 86-100% of healthy infants acquire HHV-6A as their primary HHV-6 infection (Bates *et al.*, 2009; Hall *et al.*, 2006; Kasolo *et al.*, 1997; Sjahril *et al.*, 2009). HHV-6A and HHV-6B lytically infect CD4+ T lymphocytes and undergo latency in monocytic, bone marrow progenitor cells (Luppi *et al.*, 1999; Lusso *et al.*, 1988). In addition, it has been shown *in vitro* that there are differences in cell tropism between HHV-6A and B. HHV-6A has been reported to infect *in vitro* CD8+ T cells, NK cells, γδT cells, astrocytes and

oligodendrocytes (Ahlqvist *et al.*, 2005; Donati *et al.*, 2005; Lusso *et al.*, 1991; Lusso *et al.*, 1995).

HHV-6 encodes a specific chemokine, U83 which can mediate chemoattraction for latent infection and dissemination in monocytes, but specificity and activity in subsets is not defined. HHV-6B U83B, like the human chemokine CCL2 (formerly monocyte chemotactic protein-1, MCP-1), is monospecific for CCR2, a chemokine receptor expressed on monocytes (Luttichau *et al.*, 2003). Therefore U83B can both chemoattract cellular populations for establishing latency yet also compete with CCL2 for chemokine receptor activation, thereby diverting the host's cellular responses. This specificity is in contrast to properties of homologous chemokine U83A, encoded by HHV-6A. The U83A chemokine has broad chemokine receptor specificity: CCR1, CCR4, CCR5, CCR6 and CCR8, yet does not include CCR2 (Catusse *et al.*, 2007; Dewin *et al.*, 2006). The properties of CCL2 have been shown to be essential in a number of systems, including HIV, where it is critical for mediating monocyte movement across the blood brain barrier and for subsequent correlates to neuroinflammatory disease (Buckner *et al.*, 2011; Lentz *et al.*, 2011; Williams *et al.*, 2012). During this infiltration, cells mature and become susceptible to HIV infection. HHV-6B is linked with *status epilepticus* and subsequent temporal lope epilepsy (Epstein *et al.*, 2012), where there is evidence for a role for CCL2-CCR2 signaling (van Gassen *et al.*, 2008). Therefore, we hypothesize that monocytes which express CCR2 together with CD14 and possibly CD16 are targets for HHV-6B, with U83B a key candidate for this selectivity. In this report the specificity of this chemokine is addressed and the effects on *ex vivo* human leukocytes examined. In contrast, U83A is specific for chemokine receptors, CCR5 or CCR6, which are present on dendritic cells and may affect antigen presentation by different pathways. Experiments with a spliced version of U83A, which encodes a truncated version of U83A, U83A-N, show the chemokine binding specificity is retained in the N-terminal half of

100 the molecule (Catusse *et al.*, 2007; Dewin *et al.*, 2006). Here this is further explored by
101 analysing strain variants in order to define U83B specificity for CCR2. Based on this
102 variation, synthesized peptides covering U83B-N are described to test specificity and
103 activities in mediating migration, using *ex vivo* human leukocytes to test possible effects on
104 inflammation. Specificity is defined as well as monocyte subset activation. Since
105 chemoattraction of cellular subsets can be a precursor to latent or lytic infection, this
106 specificity difference also defines a putative determinant of cellular tropism differences
107 between HHV-6A and B.

108

RESULTS AND DISCUSSION

U83 sequence variability and peptides

Prototype sequences for mature, spliced forms of U83A and U83B chemokines encoded by laboratory reference strains of HHV-6A and HHV-6B were compared (termed U83A-N and U83B-N) (Fig. 1). Additionally, comparisons of this region were made with sequences derived from clinical samples. This included 38 sequences described here from clinical strains in Zambia which were compared to 74 available on Genbank, from Japan, Germany, USA, DR Congo and Uganda, total 112. This comparison showed U83 variation between HHV-6A and B species, as previously identified (Bates *et al.*, 2009; Dewin *et al.*, 2006; French *et al.*, 1999), typified by alignments from laboratory reference strains, HHV-6A strain U1102 and HHV-6B strain Z29 (Fig. 1). This included 12 amino acid differences between U83A and U83B in the mature full-length proteins. Seven differences were present in the spliced N-terminal truncated form of the chemokine. Five of these were specific to either HHV-6A or HHV-6B. However one HHV-6B clinical strain from those characterised here from Zambia, N3, differed from the other 93 HHV-6B U83 sequences analysed. This encoded a substitution of the U83A specific lysine (K) for the U83B specific asparagine (N) at position 14 of the mature protein (Fig. 1). Such change in potential charge interactions could alter ligand-receptor interactions affecting chemokine receptor specificity. Since the N-terminal truncated spliced form still retained chemokine receptor binding specificity as shown for U83A (Catusse *et al.*, 2007; Dewin *et al.*, 2006), peptides derived from this region were examined in order to test specificity. To investigate this, peptides were synthesised corresponding to the N termini of prototype U83A and U83B (laboratory strains U1102 and Z29 respectively) and from clinical strain N3. These 17-mer peptides span 4 of the 6 differing

residues between spliced U83A and U83B and the corresponding peptides were termed NT (N-terminal): U83A-NT, U83B-NT and U83BA-NT from the clinical strain N3 (Fig. 1).

U83B-NT induces chemotaxis in *ex vivo* CCR2 positive human leukocytes

U83B-NT, U83A-NT and U83BA-NT were measured for functional activity using a chemotaxis assay in comparison to human chemokines, in physiological ranges between 0.1-10nM. Chemotaxis was first tested in both a human monocyte cell line, THP-1, which expresses CCR2 to establish the assay (Fig. 2A). Then chemotaxis assays were conducted on *ex vivo* human leukocytes expressing CCR2, derived from multiple independent healthy donors and the combined results analysed (Fig. 2B). CCR2 and CCR5 specific chemokines, CCL2 and CCL4 respectively, were used as controls. Both CCL2, 10nM positive control, and U83B-NT, 1-100nM, induced chemotaxis in the CCR2 expressing THP-1 cell line (Fig. 2A), similar to that reported for a mature U83B-Fc fusion protein (Zou *et al.*, 1999). In the *ex vivo* human PBMCs, maximal migration was similar for CCL2 and U83B-NT; significant migration was induced by U83B-NT between 0.1-10nM, with a bell shaped response curve to dilution gradients typical of chemokines. In contrast, stimulation with either U83A-NT or U83BA-NT did not induce chemotaxis of *ex vivo* PBMC which had showed positive migration to the CCL2 control (Fig. 2C). No chemotaxis was observed with U83A-NT, U83BA-NT or U83B-NT when donor cells had levels of CCR2 or CCR5 surface expression which were undetectable by flow cytometry and no response to positive control chemokines CCL2 or CCL4, specific for CCR2 or CCR5, respectively (Fig. 2D). Efficient chemotaxis by U83B-NT but not by U83A-NT or U83BA-NT, shows specificity for CCR2 by U83B resides in this N-terminal region and defines Asn-14 as a key component. Full-length purified, mature U83B effectively displaced radiolabeled CCL2 from binding to CCR2, with an EC50

of 79nM, compared to IC50 of 0.08nM for CCL2 (Luttichau *et al.*, 2003). In chemotaxis assays, mature U83B, vCCL4, was similarly efficient as CCL2 in promoting migration of CCR2 transfected murine L1.2 cell lines, albeit at higher concentrations of 100-1000nM, compared to effective concentrations for CCL2 of 0.1-10nM (Luttichau *et al.*, 2003). U83B-NT could not displace CCL2, up to 100nM (not shown) suggesting interactions at a distinct site, while the chemotaxis mediated by U83B-NT was as potent as that induced by the human chemokine CCL2, at 0.1nM-10nM. This suggests signalling is modulated by conformation of the mature virus chemokine and exposure of the U83B N-terminal peptide is important for potency. Human chemokines which bind CCR2 or CCR5 can induce rapid internalisation of the receptor within minutes (Arai *et al.*, 1997; Catusse *et al.*, 2007; Signoret *et al.*, 2005). The effects of CCL2 and U83B-NT were compared (Fig. 3). Although CCL2 induced some reduction in surface CCR2 staining, indicative of internalisation of CCR2 as described (Arai *et al.*, 1997) (Fig. 3A, B), there was no effect by U83B-NT by 10 minutes (Fig. 3C, D, in duplicate at 50nM and in quadruplicate at 1, 5, 10 and 10nM). This resembles effects of U83A on CCR5, which also induces efficient chemotaxis, but with a similar delayed receptor internalisation different from the rapid internalisation/recycling induced by human chemokines (Catusse *et al.*, 2009; Catusse *et al.*, 2007). Interestingly, CCL2 induced chemotaxis has also been reported independent of CCR2 internalisation (Arai *et al.*, 1997). The mature U83B, is monospecific for CCR2 and shows no interaction with CCR5 or other human chemokine receptors including CX3CR1 (Luttichau *et al.*, 2003). This suggests specificity for classical or intermediate monocytes.

Migrated *ex vivo* PBMC induced by U83B peptide are enriched in CCR2

In the chemotaxis assay donor PBMC bearing CCR2 could be specifically stimulated by U83B-NT (and also CCL2) and positive chemotaxis could only be observed in donors where there was a relatively high overall prevalence of CCR2 bearing cells in the PBMC population. In order to further investigate this specificity, the phenotype of the actual migrated population of *ex vivo* PBMC was characterised. Since this assay actually phenotypes the migrated population, it could be performed on donor PBMC in which the relative prevalence of CCR2+ leukocytes in the starting population from donor PBMC was lower or even a minor group. The chemotaxed cells were collected and examined by flow cytometry.

Ex vivo PBMC stimulated immediately after isolation with either U83B-NT or CCL2 in transwell chemotaxis assays showed enrichment for CCR2+ cells post-migration relative to the original PBMC population (stock cells) as well as the post-migration buffer control (Fig. 4, top panel). Similar CCR2 enrichment post-migration was shown in three further donors tested after U83B-NT and CCL2 stimulation compared to buffer only treatment (Fig. 4A and C, respectively). In these the starting population had low CCR2 expression as shown by background migration to buffer only. Even with lower CCR2 expressing subsets, U83B-NT could selectively enrich the CCR2 population. Full-length, mature U83A did not increase the prevalence of CCR2 expressing cells (Fig. 4B), When cells were cultured to increase CCR5 expression, as shown previously (Catusse *et al.*, 2009; Catusse *et al.*, 2007), treatment with U83B-NT did not increase migration of CCR5 bearing PBMCs. In contrast, there was enrichment of CCR5, but not CCR2, bearing cells after migration towards full length mature U83A (Fig. 4D), which has specificity for CCR5, but not CCR2 (Catusse *et al.*, 2007; Dewin *et al.*, 2006) . Since the migration of CCR2 and not CCR5 bearing PBMCs was increased with U83B-NT relative to the buffer-only treatment, this indicates CCR2 specificity rather than general leukocyte activation.

205

206 **Shape change assay for cellular activation induced by U83B peptide**

207 Shape change is an indicator of cellular activation and can involve alterations in cell size,
208 granularity or overall morphology as shown for CCL4 and U83A treatment of CCR5
209 expressing human leukocytes by confocal microscopy and on eosinophils treated with CCL11
210 by flow cytometry (Catusse *et al.*, 2007; Sabroe *et al.*, 1999; Signoret *et al.*, 2005). CCR5
211 cells interacting with CCL4 show internalisation of CCR5 and a decreased cellular
212 morphology, whereas CCR3 expressing eosinophils treated with cognate ligand CCL11 react
213 with morphological changes leading to increased forward scatter in flow cytometry. A similar
214 flow cytometry based assay was established using *ex vivo* PBMCs to further investigate the
215 the CCR2 specificity of U83B-NT activation, and the affected monocyte subsets (Fig. 5).
216 Shape change in response to chemokine stimulation was first compared between CCR2 and
217 CCR5 expressing cells using gating strategy is shown in Fig. 5A-D. PBMCs were stimulated
218 with chemokine or buffer only treatment control then either CCR2 or CCR5 expressing cells
219 gated on (Fig. 5A, B) and CD3 expressing and/or dead cells gated out (lineage gating, Fig.
220 5C, D). Chemokine stimulated changes in forward scatter, either increased for CCR2 or
221 decreased for CCR5, were then analysed as compared to no treatment buffer only control
222 (Fig. 5E).

223 The effects of U83B-NT were compared with those induced by stimulation with human
224 chemokines specific for CCR2 or CCR5, CCL2 or CCL4 respectively, in relation to buffer
225 only treatment (Fig. 5E). Both CCL2 and U83B-NT showed similar shape change effects in
226 increasing forward scatter relative to the buffer control in the CCR2+/CD3- population (Fig.
227 5E). In contrast, CCL4 stimulation had little effect on these CCR2+/CD3- cells, while in the
228 CCR5+/CD3- cells, CCL4 stimulation resulted in a decrease in forward scatter, consistent

with alterations in cellular morphology previously observed. There was no effect on CCR5+/CD3- PMBCs of either CCL2 or U83B-NT. This further shows the specificity of the effect of U83B-NT in activating CCR2+ PBMCs. Monocytes are a major population expressing CCR2. T-lymphocyte subsets may also express CCR2, but since CD3 expressing cells were also gated out here, it is likely that monocytes are the main population responding. Although NK or dendritic cells may also be present, these generally express CCR5 in activated forms.

U83B-NT stimulation of CCR2+CD14+CD16+ monocytic cells

CCR2 expression has been identified in CD14+CD16- classical monocytes, and is decreased or absent in non-classical CD14lowCD16+ monocytes. However, CCR2 is also expressed in the recently defined intermediate monocyte subset which is CD14+CD16+. Therefore the monocyte subsets activated by U83B-NT in the shape change assay were examined. In the donor used for the experiment in Fig 5, there were sufficient CCR2+ cells to enable analysis of the relative contribution of the different monocyte subsets to the response. Therefore, cells activated after stimulation with chemokines as indicated by the shape change assay were further analysed for monocytic markers, LPS receptor, CD14, and the FcγIII receptor, CD16. CCR2+/CD3- cells and CCR5+/CD3- cells which changed shape (increase or decrease in forward scatter profile, respectively) relative to the buffer median were assessed by flow cytometry to enable the frequency of CD14+, CD16+ populations in the increased (CCR2+CD3-) or decreased (CCR5+CD3-) forward scatter gates to be compared between chemokine and buffer only treatments (Fig. 5E). Both the U83A-NT and negative control human chemokine CCL4 (CCR5 specific) stimulation of CCR2+CD3- cells, showed no difference to the buffer-only treatment (Fig. 5E and Table 1), while both U83B-NT and the

positive control human chemokine CCL2 (CCR2 specific) induced shape change (increased forward scatter gate) and the responding population contained a higher frequency of both CD14+ and CD16+ cells, as well as dually expressing cells showing the activated cells were predominantly (>83%) CD14+ or CD16+ monocytic cells, with >77% of this population showing dual staining. This was not seen in the CCR5+CD3- CCL4 activated population, with only 0.14% CD14+CD16+ cells being present in the shape changed population (reduced forward scatter gate) (Table 1). This indicates U83B-NT can activate specifically CCR2+CD14+CD16+, intermediate monocytes.

Intermediate monocytes and non-classical monocytes, which express both CD14 and CD16, have been increasingly defined as an intrinsic subset for virus interactions and some other intracellular pathogens (Balboa *et al.*, 2011; Buckner *et al.*, 2011; Chimma *et al.*, 2009; Lentz *et al.*, 2011; Williams *et al.*, 2012). With lower expression of CD14, human CD14dim monocytes have roles in local tissue surveillance to detect nucleic acids and viruses via innate TLR7 and TLR8 pathways and appear to correlate with motile monocytes which patrol the vasculature (Cros *et al.*, 2010). In intermediate monocytes, CCR2 expression is also intermediate, yet U83B-NT can activate this subset, despite the increased CCR2 expression in classical CD14+CD16- subset, possibly indicating different CCR2 conformation or signalling in this subset. The transition to CD16 expression from classical monocyte does appear to coincide with expression of genes giving increased motility, so this could also explain this finding. In the donor used for the experiments in Fig. 5/Table 1, CCL2 also activated this subset, so this could be a donor specific finding, but still demonstrates that U83B peptide can activate the intermediate subset. Monocytes generally comprise 10% of *ex vivo* human PBMCs, and of these 85% are classical monocytes with CD14+CD16-, while the intermediate monocyte subset CD14+CD16+ is approximately 5% (Ziegler-Heitbrock *et al.*, 2010), so 0.5% of starting input PBMCs collected could have properties of this subset

susceptible to U83B activation. This limited the number of cells available for analyses of activation, particularly as CCR2 is induced in proinflammatory conditions, therefore lower or not detected in healthy donors. The conditions were only available for *ex vivo* analyses of the shape change phenotype assay in the donor indicated. It would be of interest to extend these observations to patient cohorts with inflammatory disease. The other flow cytometry and chemotaxis assays were all replicated in multiple healthy donors. A major strength of these analyses is the use of *ex vivo* cells which have not been influenced by cytokine-activated culture, therefore are most likely to represent physiologically active circulating subsets and native interactions with the virus chemokine.

The CCR2+CD14+CD16+ phenotype has also been characterised as increased in senescent cells, and can explain the increase in chronic inflammatory conditions in ageing populations including those with cardiovascular disease (Merino *et al.*, 2011; Rogacev *et al.*, 2011; Shantsila *et al.*, 2011). HHV-6B is associated with inflammatory conditions, including encephalitis and myocarditis, where it is the most frequent virus identified together with parvovirus 19 (Kuhl *et al.*, 2005a). Therefore, the U83B specificity further defined here, provide a mechanism for modulation of the inflammatory response.

Since both HHV-6A and HHV-6B have also recently been identified as integrated genomes ranging between 0.1 – 1.0% of global populations, up to 70 million people are potentially exposed to effects of these virus genes (Arbuckle *et al.*, 2010; Arbuckle & Medveczky, 2011; Morissette & Flamand, 2010). Evidence suggests the integrated HHV-6 is primarily in a latent state, but there are reports of reactivation giving placental infection (Hall *et al.*, 2010). Moreover, in the absence of other virus gene expression both HHV-6A and HHV-6B U83-N, can be expressed, encoding the spliced truncated version which includes the U83B peptide (French *et al.*, 1999). This immediate early profile suggests U83 is competent to be expressed from the genome, could be expressed from every cell, thereby enhancing chemokine

303 activities in addition to CCL2 in inflammatory disorders. Notably, CCL2 has been described
304 in both neuroinflammatory and cardiovascular pathologies and U83B with similar properties,
305 but potentially wider cellular distribution as an integrated gene could contribute to this.

306 Therefore, properties of U83B shown here are relevant both to the virus and as a virus gene
307 expressed independently as a 'human' gene. Furthermore, to our knowledge, U83B-NT, as
308 characterised here, is the smallest CCR2 specific peptide which can function potently in
309 chemotaxis. Given its small size and efficacy, it could be used as a selective agent to
310 stimulate intermediate monocytes, as a novel adjuvant for increasing vaccine efficacy due to
311 the antigen presenting features, including MHC class II expression, of this cellular subset. It
312 may also have particular applicability to recently defined prime- chemokine 'pull'
313 vaccination strategies (Shin & Iwasaki, 2012).

MATERIALS AND METHODS

Chemokine and peptide reagents. Chemokines CCL2 (MCP-1), CCL3 (MIP-1α), CCL4 (MIP-1β) and CCL5 (RANTES) were purchased in lyophilized form from Peprotech (Rocky Hill, NJ, USA) and reconstituted according to the manufacturer's instructions. 10mM aliquots of the chemokines were prepared, diluting the reconstituted peptide in Phosphate Buffered Saline (PBS), pH8. These aliquots were stored at -80°C. Working stocks (10μM) were prepared when required from these aliquots in HEPES buffered saline solution (HBSS, Sigma) with 0.1% bovine serum albumin (BSA, Sigma) and were stored at -20°C. Working stocks were discarded after two freeze-thaw cycles. Viral chemokine peptides were synthesised by Sigma-Genosys and reconstituted using the manufacturer's instructions. Briefly, chemokine was reconstituted with DMSO (Sigma) to make a 5mM stock concentration and then aliquots of 100μM and 10μM prepared using PBS/0.1% BSA and stored at -20°C. After two freeze-thaw cycles aliquots were discarded.

Polymerase chain reaction (PCR) amplification and nucleotide sequencing. HHV-6 DNA was isolated from infant sera samples collected in Zambia as part of analyses of infection effects in a nutrition intervention study as described (CIGNISstudyteam, 2010). HHV-6 U83 was PCR amplified using Gotaq green mastermix (Promega) or Pfu polymerase (New England Biosciences), as described (Bates *et al.*, 2009; French *et al.*, 1999). Outer primers U83OF/OR were used followed by a nested set, U83IF/IR: U83OF 5'AGTTAACACGACGGGAACAAC3', U83OR 5'TTGGGATGATTATGGCAAACT3', U83IF 5'GTAGGGAAAAAGACTTGTCGAA3', U83IR 5'AACCAGTATTAATGTCTTCGA3'. Gel purified DNA PCR products were sequenced using Big dye terminator 3.1 (Applied Biosystems) and run on an ABI3730 (Applied

Biosystems). Sequences were analysed using Chromas pro (Technelysium) and compared to chemokine sequences on Genbank using NCBI BLAST. Alignments were prepared using ClustalW (Chenna *et al.*, 2003) and Jalview v2.4 (Waterhouse *et al.*, 2009).

Human *ex vivo* peripheral blood mononuclear cells (PBMC) purification and culture. Whole blood was collected with 5mM EDTA (final concentration) from anonymously coded healthy adult human blood donors (LSTHM, UK), with written consent, following local phlebotomy guidelines. PBMCs were separated from whole blood using Histopaque-1077 (Sigma). PBMCs for culture were resuspended in RPMI-1640 with 10% autologous human serum, 2mM Glutamax (Fisher), 50 U/mL penicillin (Sigma), 50 µg/mL streptomycin (Sigma), plated in an ultra-low adherence flask (Corning, Corning, NY) and incubated at 37^{o}C with 5% CO_2 for 72h as described (Catusse *et al.*, 2007).

Chemotaxis assay. PBMCs at a density of $2x10^6$/ml were incubated in HBSS with 0.1% BSA and 1.7µM Calcein-AM (Invitrogen) for 30 minutes at 37°C, 5% CO_2. Cells were washed in chemotaxis buffer (HBSS/0.1% BSA), then $1.5x10^5$ cells, at a density of $3x10^6$/ml, were plated out on a Neuroprobe ChemoTX™ microchemotaxis chamber (Receptor Technologies, UK) on the filter above the lower chambers containing chemokine, peptide or buffer. The assay was then run for 90 minutes by incubation of the cell and chemokine/peptide filled microchemotaxis chamber at 37°C, 5% CO_2. Excess cells were removed from the filter and cells migrated into the lower chamber were assayed using calcein fluorescence measured with a Wallac Victor2 spectrometer (Perkin Elmer) with excitation 485nm and emission 535nm as described (Catusse *et al.*, 2007).

Flow cytometry. PBMC or THP-1 cells were stained with combinations of anti-human receptor antibodies directly conjugated to fluorescent labels. These included CCR2-phycoerythrin, PE, (FAB151P, R&D systems), CCR5-fluoroscein isothiocyanate, FITC, (FAB182F, R&D systems) CD3-pacific blue, PB, (BD Pharmagen #558124), CD14-allophycocyanin, APC (BD 555399) or CD16-PE-Cyanin7, PE-Cy7, (BD 557744) antibodies, as well as 'Dead' stain-violet with same spectrum and detected in same channel as PB (Invitrogen, L34955). PBMCs were incubated with labelled antibodies, isotype or buffer only controls for 30 minutes at 4°C, then washed with FACS buffer (PBS/0.1%BSA) followed by fixing with 2% PFA for 15 minutes prior to analysis on a FACS Calibur (Becton Dickinson). Data were analysed and compensation applied, where multicolour staining was used, with FlowJo software (Treestar).

Shape change assay. *Ex vivo* PBMCs were incubated with or without positive control human chemokines (CCL2 or CCL4), virus chemokine peptide (U83B-NT, U83A-NT, or U83BA-NT) or buffer for 90 minutes at 37^{o}C, same as for the chemotaxis assay. This was followed by centrifugation, buffer wash, then staining for multi-colour flow cytometry, using incubation with dead stain-PB and the following conjugated antibodies: CD3-PB, CCR2-PE, and CCR5-FITC, CD14-APC and CD16-PE.Cy7. Samples were run on a FACS CyAn flow cytometer (Beckman Coulter). For analyses, events were gated on flow cytometry markers (dead stain-/CD3-/CCR2+ or dead stain-/CD3-/CCR5+) then forward and side scatter profiles of these cells examined. CCR2+ or CCR5+ cells with changed forward scatter, relative to the buffer, were gated after chemokine or peptide stimulation and then further analysed for CD14 and CD16 composition by gating for CD14-APC or CD16-PE.Cy7 staining.

386 **ACKNOWLEDGMENTS**

387 We thank Carolynn Stanley, LSHTM, for phlebotomy and all blood donors at LSHTM. We
388 also thank University of London for a postgraduate research award, LSHTM for a Graduate
389 Teaching Assistant PhD scholarship (DC) and early support from the Biotechnology and
390 Biological Sciences Research Council.

REFERENCES

Adams, M. J. & Carstens, E. B. (2012). Ratification vote on taxonomic proposals to the International Committee on Taxonomy of Viruses (2012). *Arch Virol* **157**, 1411-1422.

Ahlqvist, J., Fotheringham, J., Akhyani, N., Yao, K., Fogdell-Hahn, A. & Jacobson, S. (2005). Differential tropism of human herpesvirus 6 (HHV-6) variants and induction of latency by HHV-6A in oligodendrocytes. *J Neurovirol* **11**, 384-394.

Arai, H., Monteclaro, F. S., Tsou, C. L., Franci, C. & Charo, I. F. (1997). Dissociation of chemotaxis from agonist-induced receptor internalization in a lymphocyte cell line transfected with CCR2B. Evidence that directed migration does not require rapid modulation of signaling at the receptor level. *J Biol Chem* **272**, 25037-25042.

Arbuckle, J. H., Medveczky, M. M., Luka, J., Hadley, S. H., Luegmayr, A., Ablashi, D., Lund, T. C., Tolar, J., De Meirleir, K., Montoya, J. G., Komaroff, A. L., Ambros, P. F. & Medveczky, P. G. (2010). The latent human herpesvirus-6A genome specifically integrates in telomeres of human chromosomes in vivo and in vitro. *Proc Natl Acad Sci U S A* **107**, 5563-5568.

Arbuckle, J. H. & Medveczky, P. G. (2011). The molecular biology of human herpesvirus-6 latency and telomere integration. *Microbes Infect* **13**, 731-741.

Balboa, L., Romero, M. M., Basile, J. I., Sabio y Garcia, C. A., Schierloh, P., Yokobori, N., Geffner, L., Musella, R. M., Castagnino, J., Abbate, E., de la Barrera, S., Sasiain, M. C. & Aleman, M. (2011). Paradoxical role of CD16+CCR2+CCR5+ monocytes in tuberculosis: efficient APC in pleural effusion but also mark disease severity in blood. *J Leukoc Biol* **90**, 69-75.

Bates, M., Monze, M., Bima, H., Kapambwe, M., Clark, D., Kasolo, F. C. & Gompels, U. A. (2009). Predominant human herpesvirus 6 variant A infant infections in an HIV-1 endemic region of Sub-Saharan Africa. *J Med Virol* **81**, 779-789.

Buckner, C. M., Calderon, T. M., Willams, D. W., Belbin, T. J. & Berman, J. W. (2011). Characterization of monocyte maturation/differentiation that facilitates their transmigration

across the blood-brain barrier and infection by HIV: implications for NeuroAIDS. *Cell Immunol* **267**, 109-123.

Catusse, J., Clark, D. J. & Gompels, U. A. (2009). CCR5 signalling, but not DARC or D6 regulatory, chemokine receptors are targeted by herpesvirus U83A chemokine which delays receptor internalisation via diversion to a caveolin-linked pathway. *J Inflamm (Lond)* **6**, 22.

Catusse, J., Parry, C. M., Dewin, D. R. & Gompels, U. A. (2007). Inhibition of HIV-1 infection by viral chemokine U83A via high-affinity CCR5 interactions that block human chemokine-induced leukocyte chemotaxis and receptor internalization. *Blood* **109**, 3633-3639.

Chenna, R., Sugawara, H., Koike, T., Lopez, R., Gibson, T. J., Higgins, D. G. & Thompson, J. D. (2003). Multiple sequence alignment with the Clustal series of programs. *Nucleic Acids Res* **31**, 3497-3500.

Chimma, P., Roussilhon, C., Sratongno, P., Ruangveerayuth, R., Pattanapanyasat, K., Perignon, J. L., Roberts, D. J. & Druilhe, P. (2009). A distinct peripheral blood monocyte phenotype is associated with parasite inhibitory activity in acute uncomplicated Plasmodium falciparum malaria. *PLoS Pathog* **5**, e1000631.

CIGNISstudyteam (2010). Micronutrient fortification to improve growth and health of maternally HIV-unexposed and exposed Zambian infants: a randomised controlled trial. *PLoS One* **5**, e11165.

Cros, J., Cagnard, N., Woollard, K., Patey, N., Zhang, S. Y., Senechal, B., Puel, A., Biswas, S. K., Moshous, D., Picard, C., Jais, J. P., D'Cruz, D., Casanova, J. L., Trouillet, C. & Geissmann, F. (2010). Human CD14dim monocytes patrol and sense nucleic acids and viruses via TLR7 and TLR8 receptors. *Immunity* **33**, 375-386.

Dewin, D. R., Catusse, J. & Gompels, U. A. (2006). Identification and characterization of U83A viral chemokine, a broad and potent beta-chemokine agonist for human CCRs with unique selectivity and inhibition by spliced isoform. *Journal of Immunology* **176**, 544-556.

Donati, D., Martinelli, E., Cassiani-Ingoni, R., Ahlqvist, J., Hou, J., Major, E. O. & Jacobson, S. (2005). Variant-specific tropism of human herpesvirus 6 in human astrocytes. *J Virol* **79**, 9439-9448.

Epstein, L. G., Shinnar, S., Hesdorffer, D. C., Nordli, D. R., Hamidullah, A., Benn, E. K. T., Pellock, J. M., Frank, L. M., Lewis, D. V., Moshe, S. L., Shinnar, R. C., Sun, S. & team, F. s. (2012). Human herpesvirus 6 and 7 in febrile status epilepticus: The FEBSTAT study. *Epilepsia* **doi: 10.1111/j.1528-1167.2012.03542.x**, 1528-1167.

French, C., Menegazzi, P., Nicholson, L., Macaulay, H., DiLuca, D. & Gompels, U. A. (1999). Novel, nonconsensus cellular splicing regulates expression of a gene encoding a chemokine-like protein that shows high variation and is specific for human herpesvirus 6. *Virology* **262**, 139-151.

Hall, C. B., Caserta, M. T., Schnabel, K. C., McDermott, M. P., Lofthus, G. K., Carnahan, J. A., Gilbert, L. M. & Dewhurst, S. (2006). Characteristics and acquisition of human herpesvirus (HHV) 7 infections in relation to infection with HHV-6. *J Infect Dis* **193**, 1063-1069.

Hall, C. B., Caserta, M. T., Schnabel, K. C., Shelley, L. M., Carnahan, J. A., Marino, A. S., Yoo, C. & Lofthus, G. K. (2010). Transplacental congenital human herpesvirus 6 infection caused by maternal chromosomally integrated virus. *J Infect Dis* **201**, 505-507.

Hall, C. B., Long, C. E., Schnabel, K. C., Caserta, M. T., McIntyre, K. M., Costanzo, M. A., Knott, A., Dewhurst, S., Insel, R. A. & Epstein, L. G. (1994). Human herpesvirus-6 infection in children. A prospective study of complications and reactivation. *N Engl J Med* **331**, 432-438.

Kasolo, F. C., Mpabalwani, E. & Gompels, U. A. (1997). Infection with AIDS-related herpesviruses in human immunodeficiency virus-negative infants and endemic childhood Kaposi's sarcoma in Africa. *J Gen Virol* **78 (Pt 4)**, 847-855.

Kuhl, U., Pauschinger, M., Noutsias, M., Seeberg, B., Bock, T., Lassner, D., Poller, W., Kandolf, R. & Schultheiss, H. P. (2005a). High prevalence of viral genomes and multiple viral infections in the myocardium of adults with "idiopathic" left ventricular dysfunction. *Circulation* **111**, 887-893.

Kuhl, U., Pauschinger, M., Seeberg, B., Lassner, D., Noutsias, M., Poller, W. & Schultheiss, H. P. (2005b). Viral persistence in the myocardium is associated with progressive cardiac dysfunction. *Circulation* **112**, 1965-1970.

Lentz, M. R., Kim, W. K., Kim, H., Soulas, C., Lee, V., Venna, N., Halpern, E. F., Rosenberg, E. S., Williams, K. & Gonzalez, R. G. (2011). Alterations in brain metabolism during the first year of HIV infection. *J Neurovirol* **17**, 220-229.

Luppi, M., Barozzi, P., Morris, C., Maiorana, A., Garber, R., Bonacorsi, G., Donelli, A., Marasca, R., Tabilio, A. & Torelli, G. (1999). Human herpesvirus 6 latently infects early bone marrow progenitors in vivo. *J Virol* **73**, 754-759.

Lusso, P., De Maria, A., Malnati, M., Lori, F., DeRocco, S. E., Baseler, M. & Gallo, R. C. (1991). Induction of CD4 and susceptibility to HIV-1 infection in human CD8+ T lymphocytes by human herpesvirus 6. *Nature* **349**, 533-535.

Lusso, P., Garzino-Demo, A., Crowley, R. W. & Malnati, M. S. (1995). Infection of gamma/delta T lymphocytes by human herpesvirus 6: transcriptional induction of CD4 and susceptibility to HIV infection. *J Exp Med* **181**, 1303-1310.

Lusso, P., Markham, P. D., Tschachler, E., di Marzo Veronese, F., Salahuddin, S. Z., Ablashi, D. V., Pahwa, S., Krohn, K. & Gallo, R. C. (1988). In vitro cellular tropism of human B-lymphotropic virus (human herpesvirus-6). *J Exp Med* **167**, 1659-1670.

Luttichau, H. R., Clark-Lewis, I., Jensen, P. O., Moser, C., Gerstoft, J. & Schwartz, T. W. (2003). A highly selective CCR2 chemokine agonist encoded by human herpesvirus 6. *J Biol Chem* **278**, 10928-10933.

Merino, A., Buendia, P., Martin-Malo, A., Aljama, P., Ramirez, R. & Carracedo, J. (2011). Senescent CD14+CD16+ monocytes exhibit proinflammatory and proatherosclerotic activity. *J Immunol* **186**, 1809-1815.

Morissette, G. & Flamand, L. (2010). Herpesviruses and chromosomal integration. *J Virol* **84**, 12100-12109.

Noutsias, M., Rohde, M., Goldner, K., Block, A., Blunert, K., Hemaidan, L., Hummel, M., Blohm, J. H., Lassner, D., Kuhl, U., Schultheiss, H. P., Volk, H. D. & Kotsch, K. (2011). Expression of functional T-cell markers and T-cell receptor Vbeta repertoire in endomyocardial biopsies from patients presenting with acute myocarditis and dilated cardiomyopathy. *Eur J Heart Fail* **13**, 611-618.

Rogacev, K. S., Seiler, S., Zawada, A. M., Reichart, B., Herath, E., Roth, D., Ulrich, C., Fliser, D. & Heine, G. H. (2011). CD14++CD16+ monocytes and cardiovascular outcome in patients with chronic kidney disease. *Eur Heart J* **32**, 84-92.

Sabroe, I., Hartnell, A., Jopling, L. A., Bel, S., Ponath, P. D., Pease, J. E., Collins, P. D. & Williams, T. J. (1999). Differential regulation of eosinophil chemokine signaling via CCR3 and non-CCR3 pathways. *J Immunol* **162**, 2946-2955.

Schmidt-Hieber, M., Schwender, J., Heinz, W. J., Zabelina, T., Kuhl, J. S., Mousset, S., Schuttrumpf, S., Junghanss, C., Silling, G., Basara, N., Neuburger, S., Thiel, E. & Blau, I. W. (2011). Viral encephalitis after allogeneic stem cell transplantation: a rare complication with distinct characteristics of different causative agents. *Haematol-Hematol J* **96**, 142-149.

Seeley, W. W., Marty, F. M., Holmes, T. M., Upchurch, K., Soiffer, R. J., Antin, J. H., Baden, L. R. & Bromfield, E. B. (2007). Post-transplant acute limbic encephalitis: clinical features and relationship to HHV6. *Neurology* **69**, 156-165.

Shantsila, E., Wrigley, B., Tapp, L., Apostolakis, S., Montoro-Garcia, S., Drayson, M. T. & Lip, G. Y. (2011). Immunophenotypic characterization of human monocyte subsets: possible implications for cardiovascular disease pathophysiology. *J Thromb Haemost* **9**, 1056-1066.

Shin, H. & Iwasaki, A. (2012). A vaccine strategy that protects against genital herpes by establishing local memory T cells. *Nature* **491**, 463-467.

Signoret, N., Hewlett, L., Wavre, S., Pelchen-Matthews, A., Oppermann, M. & Marsh, M. (2005). Agonist-induced endocytosis of CC chemokine receptor 5 is clathrin dependent. *Mol Biol Cell* **16**, 902-917.

Sjahril, R., Isegawa, Y., Tanaka, T., Nakano, K., Yoshikawa, T., Asano, Y., Ohshima, A., Yamanishi, K. & Sugimoto, N. (2009). Relationship between U83 gene variation in human herpesvirus 6 and secretion of the U83 gene product. *Arch Virol* **154**, 273-283.

van Gassen, K. L., de Wit, M., Koerkamp, M. J., Rensen, M. G., van Rijen, P. C., Holstege, F. C., Lindhout, D. & de Graan, P. N. (2008). Possible role of the innate immunity in temporal lobe epilepsy. *Epilepsia* **49**, 1055-1065.

Waterhouse, A. M., Procter, J. B., Martin, D. M. A., Clamp, M. & Barton, G. J. (2009). Jalview Version 2--a multiple sequence alignment editor and analysis workbench. . *Bioinformatics (Oxford, England)* **25**, 1189-1191.

Williams, D. W., Eugenin, E. A., Calderon, T. M. & Berman, J. W. (2012). Monocyte maturation, HIV susceptibility, and transmigration across the blood brain barrier are critical in HIV neuropathogenesis. *J Leukoc Biol* **91**, 401-415.

Wong, K. L., Tai, J. J., Wong, W. C., Han, H., Sem, X., Yeap, W. H., Kourilsky, P. & Wong, S. C. (2011). Gene expression profiling reveals the defining features of the classical, intermediate, and nonclassical human monocyte subsets. *Blood* **118**, e16-31.

Zawada, A. M., Rogacev, K. S., Rotter, B., Winter, P., Marell, R. R., Fliser, D. & Heine, G. H. (2011). SuperSAGE evidence for CD14++CD16+ monocytes as a third monocyte subset. *Blood* **118**, e50-61.

Zerr, D. M., Fann, J. R., Breiger, D., Boeckh, M., Adler, A. L., Xie, H., Delaney, C., Huang, M. L., Corey, L. & Leisenring, W. M. (2011). HHV-6 reactivation and its effect on delirium and cognitive functioning in hematopoietic cell transplantation recipients. *Blood* **117**, 5243-5249.

Zerr, D. M., Meier, A. S., Selke, S. S., Frenkel, L. M., Huang, M. L., Wald, A., Rhoads, M. P., Nguy, L., Bornemann, R., Morrow, R. A. & Corey, L. (2005). A population-based study of primary human herpesvirus 6 infection. *N Engl J Med* **352**, 768-776.

Ziegler-Heitbrock, L., Ancuta, P., Crowe, S., Dalod, M., Grau, V., Hart, D. N., Leenen, P. J., Liu, Y. J., MacPherson, G., Randolph, G. J., Scherberich, J., Schmitz, J., Shortman, K., Sozzani, S., Strobl, H., Zembala, M., Austyn, J. M. & Lutz, M. B. (2010). Nomenclature of monocytes and dendritic cells in blood. *Blood* **116**, e74-80.

Zou, P., Isegawa, Y., Nakano, K., Haque, M., Horiguchi, Y. & Yamanishi, K. (1999). Human herpesvirus 6 open reading frame U83 encodes a functional chemokine. *J Virol* **73**, 5926-5933.

FIGURE LEGENDS

554 **Fig. 1. U83 peptide sequences based on HHV-6A and HHV-6B clinical strains.**
555 Alignment of the amino acid sequences of the mature, spliced truncated form of U83, U83-N,
556 shown for HHV-6A, laboratory strain U1102, HHV-6B, laboratory strain Z29, and 38 clinical
557 strains analysed here in comparison to 74 strains available on NCBI. Those in bold and
558 prefaced by z are from Zambia and compared to representative clinical strains from previous
559 analyses (French *et al.*, 1999; Sjahril *et al.*, 2009). CD is a reference UK strain. The *
560 indicates amino acid differences. HHV-6A and HHV-6B strains are shown together, with
561 total numbers analysed indicated. The HHV-6B clinical strain N3 is shown separately as it
562 had a single substitution Asn-Lys14 only found in the HHV-6A strains. This substitution is
563 marked with an additional *. 17-mer peptides were derived from U83A and U83B N-terminal
564 regions and labelled U83A-NT and U83B-NT. To compare the effect of the Asn-Ly14
565 change between HHV-6A and HHV-6B U83, U83B-NT had a Gly-Cys3 substitution. The
566 HHV-6B clinical strain N3 peptide was labelled U83BA-NT.

567

568 **Fig. 2. Chemotaxis induced by U83B-NT.** Chemotactic index is calculated relative to buffer
569 only treatment which shows the background migration. This is given a value of 1, which
570 allows comparison between multiple assays; this cut-off is shown by the dotted line. (A.)
571 THP-1 human monocyte cell line expressing CCR2 (by flow cytometry), showing chemotaxis
572 to CCL2 and U83 peptide by flow cytometry assay using pooled cells (from 3 wells per
573 column), representative of two independent cultures. (B-D) Migration of *ex vivo* human
574 PBMC to stimulus in microchemotaxis chambers: (B.) CCR2 expressing *ex vivo* human
575 PBMC, show chemotaxis to CCL2 and U83B peptide; results for chemokine treatment were

combined from 4 donors using one way ANOVA with Dunnett's multiple comparison test for statistical significance versus control buffer-only treatment, * $p<0.05$, ** $p<0.01$; (C.) U83A-NT or U83BA-NT do not induce chemotaxis in *ex vivo* human PBMCs expressing CCR2 which respond to CCL2; results were combined from 3 donors as above. (D.) No chemotaxis relative to buffer only treatment in *ex vivo* PBMC which had no response to CCL2 or CCL4 and no expression of CCR2 or CCR5 by flow cytometry, five donors.

Fig. 3. CCL2 but not U83B-NT induces reduction in surface CCR2. Internalisation assay was conducted by measurement of any reductions in CCR2 surface staining after chemokine stimulation. THP-1 cells were treated with chemokine or buffer only control for 10 min then surface expression of CCR2 was assayed by flow cytometry. (A.) Control experiment without any incubation. The dotted line shows the no staining control. The grey shading indicates staining with the isotype control for the CCR2-PE antibody. The solid black line shows staining with CCR2-PE antibody indicating CCR2 expression on almost all cells. (B.) Cells were treated with CCL2 , thick black solid and thick dotted lines, or buffer only control, thin grey and thin dotted lines, for 10 min. CCL2 treatment resulted in lower levels of CCR2 staining. Results shown in duplicate of two independent experiments. (C.) Cells were treated with buffer only control, thin grey line, or with U83B-NT 50nM, thick black line, which had no effect on CCR2 surface staining. (D.) In a duplicate assay, cells were treated with different dilutions of U83B-NT, 1 , 5, 10, 20 and 50nM, and compared to buffer only control. There is no evidence of a reduction in surface CCR2 at any concentration of U83B-NT.

Fig. 4. Cells chemotaxed by U83B-NT are enriched for CCR2 bearing cells. Human *ex vivo* PBMC, stock cells expressing CCR2, which migrated though a 5μm filter during a 90

minute incubation with chemokine or buffer only treatment were collected post migration and stained separately for CCR2 or CCR5 using antibodies conjugated with fluorescent tags (PE and FITC respectively). The top panel demonstrates the assay set up with ex vivo PBMC from a representative donor. The four graphs show the prevalence of the CCR2 staining of the starting PBMC population compared to the cells that had undergone migration after treatment with chemokines U83B-NT, CCL2 or buffer only. The light grey histograms show the staining with an isotype control antibody and the solid line, clear histogram shows staining with an antibody to CCR2. Y-axes show cell counts (expressed as % Max, the percentage of the maximum number of cells) (A-D) Ex vivo PBMC from three further donors were then tested and the prevalence of CCR2 or CCR5 bearing cells which have migrated after chemokine stimulation (solid line, clear histogram) was compared to that of background migration after buffer only treatment (dark grey histogram). (A.) U83B-NT 1nM, (B.) U83A 1nM, and (C.) CCL2 10nM incubation. In (D) PBMC were cultured 3 days in non-adherent flasks to induce CCR5 expression, then treated with U83A as above.

Fig. 5. Shape change assay further defines U83B-NT CCR2 specificity.

Cells were stimulated with human chemokines, CCR2 specific CCL2 or CCR5 specific CCL4, virus chemokine U83B-NT or buffer for 90 minutes and then stained for cell markers. In this assay cells were stained for: CCR2 (PE, for gating CCR2 expressing cells), CCR5 (FITC, for gating in CCR5 expressing cells), CD3 (pacific blue, PB, for gating out T cells), Dead cell stain (PB analogue, for gating out dead cells), CD14 (APC, For gating monocytic cells), CD16 (PE-Cy7, for gating cells bearing this Fc receptor). In order to define chemokine specific responses to chemokine receptors on the cell surface, cell populations were first defined by chemokine receptor expression, either CCR2 or CCR5, which were

gated in separately to be able to compare their responses. Next the CD3+/dead cells were gated out. Finally, the shape change effect on chemokine stimulated cells was evaluated by changes in forward scatter relative to the no treatment buffer only control.

The flow cytometry gating strategy is summarised in (A-D). The grey histogram shows the fluorescence of unstained cells, and the black line cells stained cells. (A.) Identification of chemokine receptor positive cells, CCR2 or CCR5, within the total PBMC population (shown here for CCR2-PE). The gate used to delineate CCR2+ cells is indicated. CCR5+ cells were separately gated for comparison (CCR5-FITC). (B.) Dot plot showing the CCR2+ gated population. (C.) Next, within either the CCR2 or CCR5 gated populations, cells were gated out which stained for CD3 or were dead cells (CD3- PB). Similar gating was also performed with the CCR5+ population. (D.) Dot plot showing the live CCR2+CD3- gated population. (E.) Effects on forward scatter of chemokine treatment (black line) compared here to no treatment buffer only control (grey tint) on cells expressing CCR2+CD3- or CCR5CD3- cells identified as described above. Cells were stimulated with chemokines as indicated U83B-NT 1nM, CCL2 10nM, CCL4 10nM, or buffer only. In the left panels cells expressing CCR2 respond to specific chemokine stimulation by increases in forward scatter, a larger, more granular morphology, as shown for both CCL2 and U83B-NT stimulation relative to the buffer. In the right panels cells expressing CCR5 respond only to specific chemokine CCL4 stimulation showed by decreases in forward scatter, acquisition of a smaller, less granular morphology, relative to buffer. Cells were then gated (black arrows) on the increased or decreased forward scatter profiles relative to the buffer control histogram median and the relative prevalence of CD14 or CD16 cell surface marker in the shape-changed population was further determined (Table 1).

Table 1.

Frequency of $CD14^+$ $CD16^+$ monocytes in chemokine stimulated $CCR2^+$ $CD3^-$ or $CCR5^+$ $CD3^-$ *ex vivo* human PBMCs relative to buffer in shape change assay

	CCR2+CD3-			CCR5+CD3-		
Stimulation	CD14 %	$CD16^+$ %	$CD14^+$ $CD16^+$ %	$CD14^+$ %	$CD16^+$ %	$CD14^+$ $CD16^+$ %
Buffer	60.9	61.9	53.4	3.6	0.6	0.32
CCL4	65.3	65.8	57.1	1.4	0.4	0.14
CCL2	85.1	88.3	82.2	3.0	0.7	0.29
U83A-NT	67.5	68.4	62.9	4.1	0.7	0.34
U83B-NT	83.3	84.0	77.3	6.5	1.1	0.58

Fig. 1.

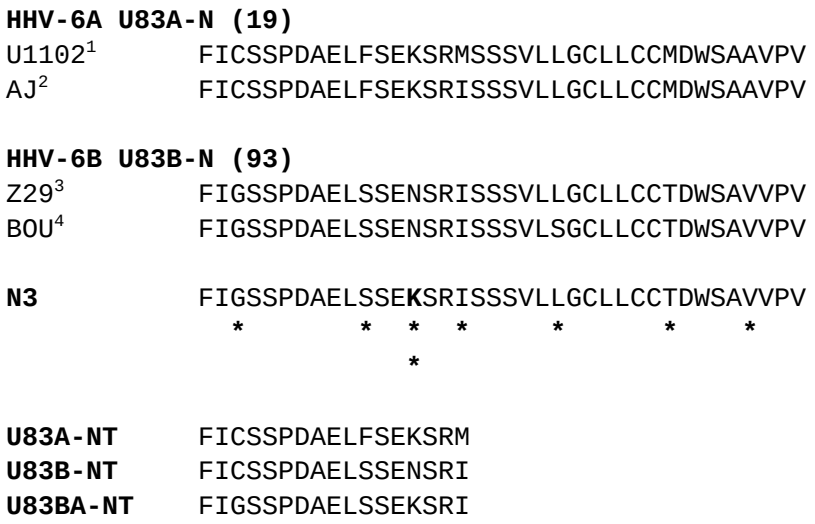

[1]U1102 is same as Z27, Z5, GS, DA, CO7, **621**, **N25, C2, 35, 184, 538**
[2]AJ is the same as Z23, Z59, 5628-5-15
[3]z29 is same as HST, MBE, HT, ES16, BT499, 16-2-41, HST, ES17, BT552, **37, 39**, **N2**, **N3, N5, N8, N9, N11, N12, N13, N15, N17, N18, N19, N22, N23, N25B, N26, N28, N33**
[4]BOU is same as z3, z12, z13, z14, z25, Z317, AB69, St.W, BT348, BT344, ES11, **N35, CD**

Fig. 2.

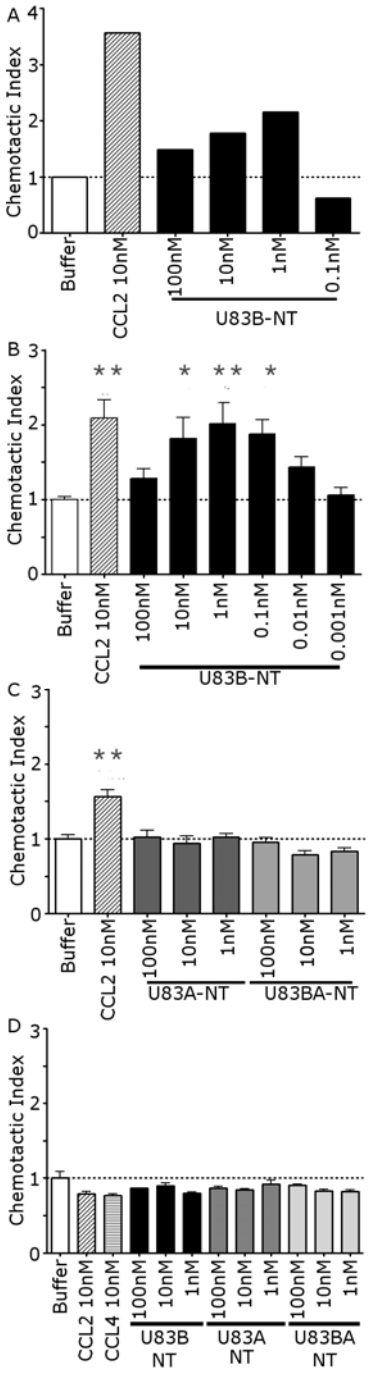
A
Chemotactic Index
Buffer
CCL2 10nM
100nM
10nM
1nM
0.1nM
U83B-NT
B
Chemotactic Index
Buffer
CCL2 10nM
100nM
10nM
1nM
0.1nM
0.01nM
0.001nM
U83B-NT
C
Chemotactic Index
Buffer
CCL2 10nM
100nM
10nM
1nM
100nM
10nM
1nM
U83A-NT
U83BA-NT
D
Chemotactic Index
Buffer
CCL2 10nM
CCL4 10nM
100nM
10nM
1nM
100nM
10nM
1nM
100nM
10nM
1nM
U83B NT
U83A NT
U83BA NT

Fig. 3

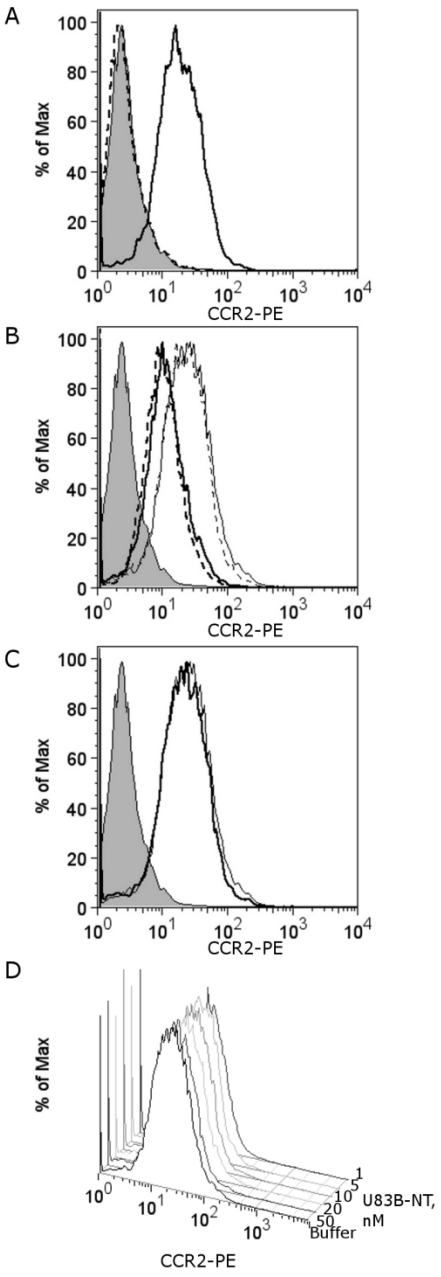

Fig. 4

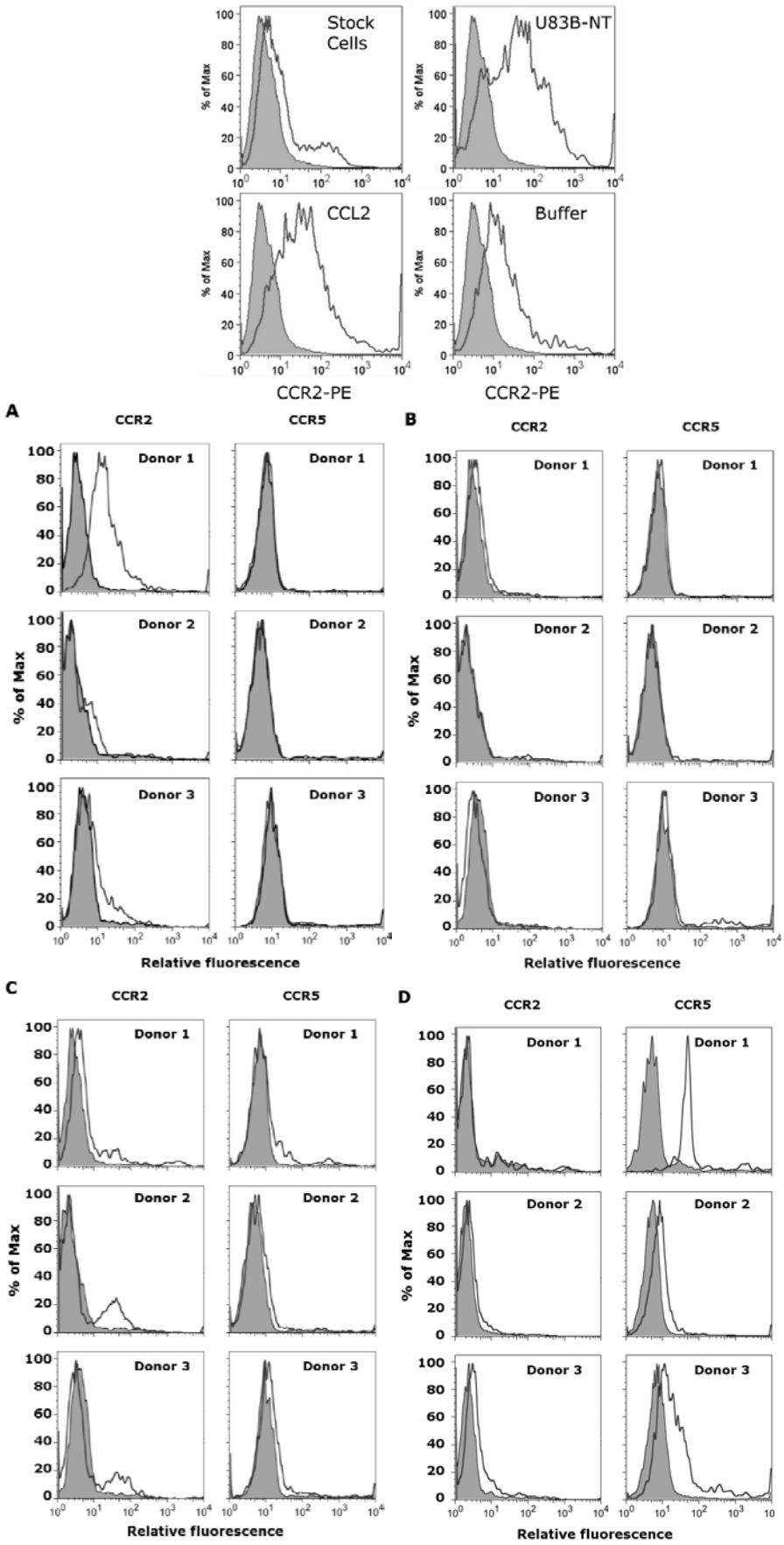
Stock Cells
U83B-NT
CCL2
Buffer
% of Max
CCR2-PE
A
B
C
D
CCR2
CCR5
Donor 1
Donor 2
Donor 3
Relative fluorescence

Fig. 5

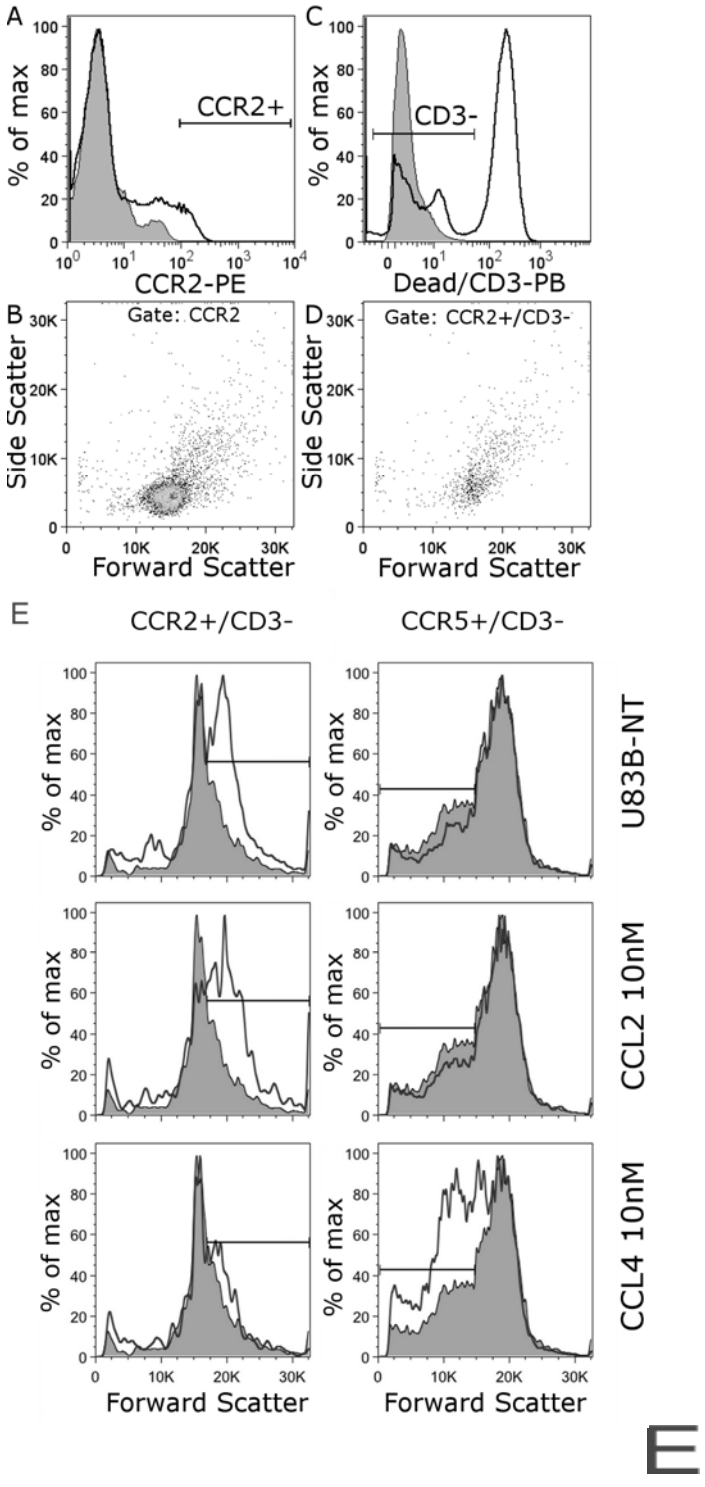
A
% of max
CCR2+
CCR2-PE
C
% of max
CD3-
Dead/CD3-PB
B
Gate: CCR2
Side Scatter
Forward Scatter
D
Gate: CCR2+/CD3-
Side Scatter
Forward Scatter
E
CCR2+/CD3-
CCR5+/CD3-
U83B-NT
CCL2 10nM
CCL4 10nM
% of max
Forward Scatter

646